Ore Geology Reviews 129 (2021) 103865

Contents lists available at ScienceDirect

Ore Geology Reviews

journal homepage: www.elsevier.com/locate/oregeorev

Review

Three late-Mesozoic fluorite deposit belts in southeast China and links to subduction of the (paleo-) Pacific plate

Haibo Yan [a,b,c], Xing Ding [a,c,*], Mingxing Ling [a], Congying Li [d,e], Daniel E. Harlov [f,g,h], Weidong Sun [d,e,*]

[a] State Key Laboratory of Isotope Geochemistry, Guangzhou Institute of Geochemistry, Chinese Academy of Sciences, Guangzhou 510640, China
[b] CAS Key Laboratory of Mineralogy and Metallogeny, Guangzhou Institute of Geochemistry, Chinese Academy of Sciences, Guangzhou 510640, China
[c] University of the Chinese Academy of Sciences, Beijing 100049, China
[d] Laboratory for Marine Mineral Resources, Qingdao National Laboratory for Marine Science and Technology, Qingdao 266237, China
[e] Center of Deep Sea Research, Institute of Oceanography, Chinese Academy of Sciences, Qingdao 266071, China
[f] Deutches GeoforschungsZentrum, Telegrafenberg, 14473, Potsdam, Germany
[g] Department of Geology, University of Johannesburg, P.O. Box 524, Auckland Park 2006, South Africa
[h] School of Earth Resources, China University of Geosciences, Wuhan 430074, China

ARTICLE INFO

Keywords:
Fluorite deposit
Plate subduction
Pacific plate
Fluorine
Slab rollback

ABSTRACT

Rocks and ore deposits in subduction zones can provide clues to material cycling and related subduction processes. Here we demonstrate, based upon a new data compilation from more than 240 late-Mesozoic fluorite deposits in southeast China that most of them can be divided into three fluorite deposit belts (FDB) with distinct ages and orientations. The two older inland FDB with a NE-SW orientation were formed at 165–150 Ma and 150–130 Ma, respectively, whereas the younger coastal FDB, roughly perpendicular to the others, was generated at 110–70 Ma. The temporal-spatial distributions of the FDB are compatible with the subduction of the (paleo-) Pacific plate. We propose that the genesis of the earlier two inland FDB was due to northeastward slab rollback during low-angle subduction, while formation of the coastal FDB resulted mainly from high-angle northwestward hot/warm subduction. Large amounts of F, mainly derived from the decomposition of phengite (±apatite) in the subducted slabs, could be transported into the overlying crust via F-rich fluids and alkalic magmas. Subsequently, extensive crustal magmatism and fluid activities associated with subduction further concentrate F from the magmas and/or wall-rocks and facilitate fluorite mineralization. This study provides new insights into the interaction between the subducting (paleo-) Pacific plate and overlying eastern Eurasian continent in the late Mesozoic. It also highlights the potential genetic association of F transport/deposition with plate subduction that could be a common phenomenon in ancient and modern subduction zones.

1. Introduction

Plate subduction is one of the most important processes for mass transfer and material cycling on Earth. It not only fertilizes and alters the Earth's interior, but also facilitates the nucleation and growth of the continental crust, which subsequently generates a large fraction of magmatic rocks and mineral deposits (Anderson, 1989; Tatsumi, 2005; Sun et al., 2012). Due to it's large scale and slow timescales, the subduction process is difficult to study directly. Thus, the rocks and mineral deposits associated with plate subduction can be used as a tracer to decipher both ancient and modern plate subduction processes, which in turn can provide information on the subduction age, angle, and style, as well as the kinematics involved in subduction (Stern, 2004; Zhou et al., 2006; Doglioni et al., 2007; Li et al., 2019; Liu et al., 2019a, 2019b).

South China has been influenced by subduction of the (paleo-) Pacific plate since the Mesozoic, resulting in large scale magmatism and polymetallic mineralization (Zhou and Li, 2000; Zhou et al., 2006; Li and Li, 2007; Sun et al., 2007, 2010; Wang et al., 2011; Hu and Zhou, 2012; Li et al., 2012; Mao et al., 2013; Ding et al., 2015; Chen et al., 2016a; Zhao et al., 2017; Dmitrienko et al., 2018; Hong et al., 2018). The

* Corresponding authors at: State Key Laboratory of Isotope Geochemistry, Guangzhou Institute of Geochemistry, Chinese Academy of Sciences, Guangzhou 510640, China (X. Ding). Laboratory for Marine Mineral Resources, Qingdao National Laboratory for Marine Science and Technology, Qingdao 266237, China (W. Sun).
E-mail addresses: xding@gig.ac.cn (X. Ding), weidongsun@qdio.ac.cn (W. Sun).

https://doi.org/10.1016/j.oregeorev.2020.103865
Received 18 March 2020; Received in revised form 5 October 2020; Accepted 16 October 2020
Available online 10 November 2020

consensus regarding subduction processes is that since the Cretaceous the northwestward subduction of the Pacific plate has dominated the formation of igneous rocks and mineral deposits, as well as shaped the present tectonic framework in South China. However, the subduction direction and style of the (paleo-) Pacific plate before the Cretaceous are still a subject of debate. This includes the different interpretations regarding northwestward subduction (Zhou et al., 2006; Li and Li, 2007; Mao et al., 2013), southwestward subduction (Sun et al., 2007; Wang et al., 2011; Liu et al., 2018a), westward subduction (Li et al., 2019), as well as low-angle subduction (Zhou and Li, 2000; Liu et al., 2019b), flat-slab subduction (Li and Li, 2007; Li et al., 2012), and high-angle subduction (Hong et al., 2018).

Globally, fluorite deposits are widely distributed on all the continents (Fig. 1). They are mostly associated with magmatic rocks with relatively high F contents and sometimes accompany rare or rare earth metal deposits (Bailey, 1977; Huang et al., 2007; Graupner et al., 2015; Xie et al., 2015). Although a single fluorite deposit likely can result from crustal non-magmatic, epigenetic, hydrothermal fluid activities (Levresse et al., 2003; Munoz et al., 2005; Camprubí, 2013; Pei et al., 2017; González-Partida et al., 2019) or from magmatic-hydrothermal fluid activities (Strong et al., 1984; Williams-Jones et al., 2000; Deng et al., 2015), large-scale contemporaneous fluorite deposits distributed along a line or belt are usually regarded as a product of plate subduction or continental rifting (Alstine Van, 1976; Lamarre and Hodder, 1978). The circum-Pacific region hosts more than 40% of the world's fluorite reserves (USGS, 2019), which were mostly generated in the Mesozoic or Cenozoic and display apparent linear or belt arrangements approximately parallel to the margins of the subduction zones (Fig. 1). It also suggests the link between formation of a fluorite deposit belt and plate subduction.

China has over 13.5% of the known world reserve of fluorite deposits (USGS, 2019), most of which are located in the circum-Pacific region. Compared to other polymetallic deposits, however, the distribution and genesis of fluorite deposits in China has been poorly studied. Given that fluorite deposits associated with plate subduction are generally linear or zonal in distribution and lie roughly parallel to the margin of the spatially-associated subduction zone, their zonation, ages, and other geochemical characteristics might therefore be indicative of the subduction processes. In this paper, we present geographical, geological, and geochronological information from a new systematic data compilation of more than 240 late-Mesozoic fluorite deposits in southeast China in order to document their temporal and spatial distribution, and then explore a possible link between the genesis of these fluorite deposits and the subduction process of the (paleo-) Pacific plate. This study, on the one hand, demonstrates that the fluorite deposits with a linear or belt distribution can be a useful tracer for determining the style of the subduction process. On the other hand, it also suggests that changes in the subduction style, likely involving subduction direction, angle, and kinetic process, have to be taken into account, especially when reconstructing the evolution of the moving plate and determining the tectonic and/or geochemical processes involved during plate subduction.

2. Geological background

Southeast China is located in the southeastern corner of the South China Block (SCB), which represents the merger of the Yangtze Block, the Cathaysia Block, and other micro-plates before the Mesozoic (Gilder et al., 1991; Metcalfe, 2013; Li et al., 2019). In the Mesozoic, southeast China underwent two important tectonic events, the early Mesozoic Indosinian orogeny (250–205 Ma) and the late Mesozoic Yanshanian orogeny (205–65 Ma). The former was related to the closure of the Tethys Ocean and subsequent collision between the Indochina Block and the SCB, while the latter was dominated by the subduction of the (paleo-) Pacific plate (Zhou et al., 2006; Sun et al., 2007; Ding et al., 2015). These two tectonic events led to the formation of Indosinian granitoids as well as the massive Yanshanian intrusion and associated volcanic rocks, with a total outcrop area of ~218,000 km^2 (Zhou et al., 2006). The Yanshanian volcanic rocks are mainly exposed in coastal areas, while the intrusive rocks are mostly distributed in the interior of southeast China, with systematically decreasing ages towards the coast (Zhou and Li, 2000). The two events shaped the modern basin and range tectonic framework as well as a series of thrusts and ductile shear zones in southeast China (Li and Li, 2007; Shu et al., 2009; Dmitrienko et al.,

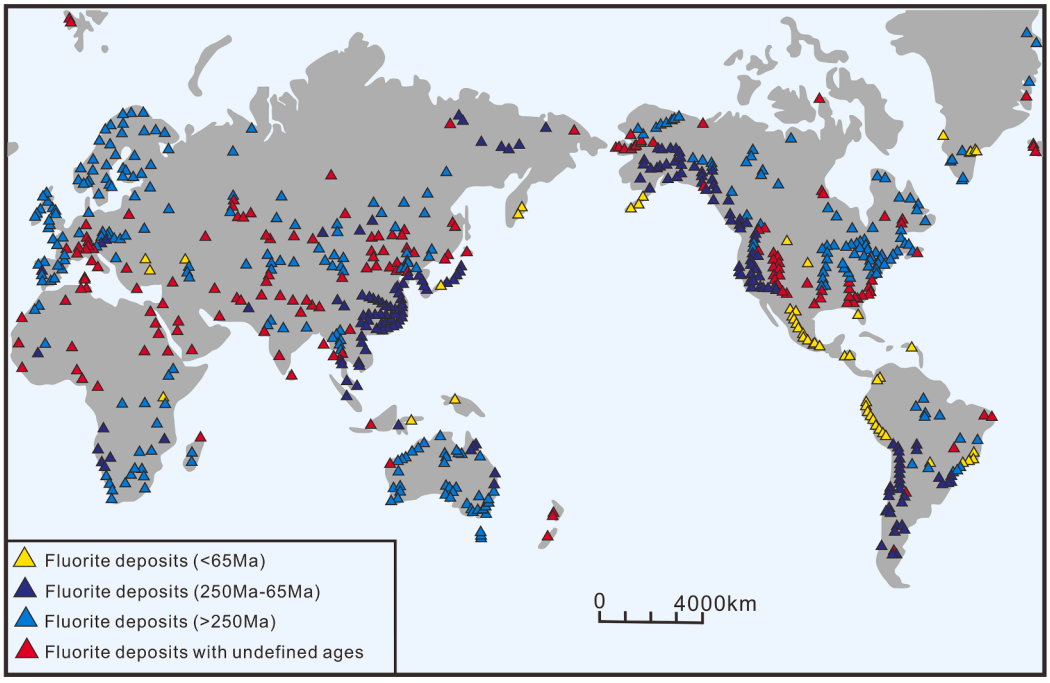

Fig. 1. The temporal and spatial distribution of fluorite deposits in the world showing that most of the fluorite deposits are located in the ancient or modern plate margin. The data are from the IMA Database of Mineral Properties (http://rruff.info/ima/).

2018; Li et al., 2019).

There are four large, deep fault zones distributed across the SCB, i.e. the Changle-Nanao Fault (CNF), the Zhenghe-Dapu Fault (ZDF), the Ganjiang Fault (GF), and the Shaoxing-Jiangshan-Pingxiang Fault (SJPF). The SJPF is considered to be the suture between the Yangtze Block and the Cathaysia Block (Gilder et al., 1991), and separates the Jiangnan Neoproterozoic orogen from the Wuyishan early Paleozoic orogen (Shu et al., 2009). The ZDF marks the approximate divide between the Wuyishan orogen and the late Mesozoic volcanic-sedimentary basins in the coastal area. The GF separates the late Mesozoic volcanic-sedimentary basins from the late Mesozoic non-volcanic basins. Lastly, the CNF is a sinistral ductile shear zone that formed in the early Cretaceous likely due to subduction of the paleo-Pacific plate (Shu et al., 2009).

3. Geology and distribution of late-Mesozoic fluorite deposits

3.1. Geographical and geological characteristics

Southeast China, particularly Zhejiang, Fujian, Jiangxi, Hunan, Guangdong, and Guangxi provinces, is located in the western circum-Pacific region. Geographical and geological information from published literature for more than 240 late-Mesozoic fluorite deposits and related rocks in southeast China were collected and compiled in this study (Table S1).

The fluorite deposits are unevenly distributed in the six provinces of southeast China. Zhejiang contains 120 fluorite deposits, including 42 large (≥1Mt) and 77 medium (>0.2 Mt, <1 Mt) or small (<0.2 Mt) deposits, such as the Tawu and Gengcun fluorite deposits. These deposits spread from the west and central to the south of Zhejiang. Fujian has 41 fluorite deposits, comprising 8 large and 33 medium or small, most of which are located in the Wuyi Mountain of western Fujian and less in central Fujian. The Changkou and Shangxiakong fluorite deposits are hereby considered to be the most representative ones in the province. In Jiangxi, 57 fluorite deposits are mainly distributed in Xingguo, Longnan, and Huichang counties, including 12 large and 45 medium or small deposits, such as Junmenling and Shuiweishan. In contrast, Hunan, Guangdong, and Guangxi provinces contribute fewer but much higher reserves of fluorite than other provinces. Hunan has 14 fluorite deposits (8 large and 6 medium or small), which occur mainly in Chenzhou and Hengyang in southern Hunan. The Shuangjiangkou and Tangqian deposits are considered to be the most representative among them. Six large and 4 medium or small fluorite deposits are located in eastern and northern Guangdong, such as the Jingkanshan and Zhongdong deposits. Only 5 late-Mesozoic fluorite deposits are found in Guangxi, most of which are distributed in Ziyuan county, North Guangxi, such as the Shuanghuajiang and Jiaozishui deposits.

The fluorite deposits in Southeast China display comparable geological characteristics and are mostly associated with intrusive and volcanic rocks that are widely distributed in the foreland or passive marginal basin of the Yangtze block as well as the Wuyi-Yunkai and Nanling orogens (Chen et al., 1991; Ling et al., 1999; Qiu et al., 1999; Li et al., 2003; Wang et al., 2005a, 2005b, 2011; Fang et al., 2020). The fluorite deposits in the basins of central Zhejiang and Jiangxi formed in or adjacent to late-Mesozoic felsic volcanic rocks and granitoids (Table S1). These rocks usually overlie the Precambrian folded basement and are partially covered by younger sedimentary rocks or sediments (Li and Wang, 1996; Han et al., 2012). The deposits consist mainly of fluorite and quartz and occur within fracture zones with veined, massive, and lamellar textures (Wang et al., 2014). The distribution of the deposits is controlled by regional NE- or NW-strike faults (Chen and Qiu, 2013). Previous studies demonstrated that most of these fluorite deposits were formed after leaching from wall rocks by low-temperature hydrothermal fluids, in which felsic magmas supplied the heat and a portion of the ore-forming materials (Cao, 1995; Liu et al., 2012). However, a few other fluorite deposits have been proposed to be derived from metamorphic volcanic or sedimentary rocks in the basement, unrelated to any magmatic activities (Xia et al., 2010; Han et al., 2012). Their genesis is similar to those of carbonate-hosted Pb-Zn ore deposits or MVT Pb-Zn-F-Ba deposits (González-Sánchez et al., 2009; Zhang et al., 2019, 2020).

The fluorite deposits in the Wuyi-Yunkai orogen spread over southern Zhejiang, eastern Jiangxi, western Fujian, and Guangdong provinces while those in the Nanling orogen are distributed through northern Guangxi, southern Hunan, northern Guangdong to the southern Jiangxi. These deposits are commonly hosted by Mesozoic granitoids, such as Mesozoic highly-evolved granites and alkaline rocks (e.g., A-type granites and syenites), in addition to a few subvolcanic rocks, Jurassic tuffs, and Precambrian metamorphic and sedimentary rocks (Table S1) (Wang et al., 2005a, 2014; Chen et al., 2016b). The mineral deposits, especially in the Nanling orogen, are veined or lenticular, generally accompanied by another metallic mineralization (Wang et al., 1987, 2014; Lu et al., 2003; Yuan et al., 2008, 2015; Zhang and Hu, 2012; Zhu et al., 2012), such as the Shizhuyuan W-Sn-Bi-Mo-F association (Wang et al., 1987; Lu et al., 2003), the Qitianling Sn-W-Pb-Zn-F association (Yuan et al., 2008; Xie et al., 2015), the Xihuashan Scheelite-fluorite and quartz-fluorite associations (Maruéjol et al., 1990), and the Taolin Pb-Zn-fluorite-barite association (Zhang and Hu, 2012). It has been proposed that the fluorite deposits in the orogens are genetically associated with the nearby Mesozoic magmatic rocks, most of which supply a large amount of ore-forming material (Cao, 1987; Li and Wang, 1996; Wang et al., 2005a, 2005b, 2014). For example, in the Nanling orogen, Xie et al. (2015) demonstrated that Sn-Ti-F mineralization in the Qitianling District was derived from highly-evolved topaz rhyolites. The giant Shizhuyuan fluorite deposit and associated W-Sn-Bi-Mo mineralization is also believed to have a close relationship with 155–158 Ma highly-evolved granites (Lu et al., 2003).

3.2. Temporal and spatial distribution of fluorite deposits

Age dating of fluorite mineralization currently consists of direct and indirect methods. Direct dating of fluorite has been carried out by means of Sm-Nd isochron, fission-track, and U-Th/He radiometric or isotopic methods (Li and Jiang, 1989; Chesley and Liu, 1992; Munoz et al., 2005; Pi et al., 2005). Indirect dating provides an estimation on the age of fluorite mineralization by determining the formation age of minerals associated with fluorite, such as molybdenite Re-Os isochron ages (Mao et al., 1999), mica or galena Rb-Sr isochron ages (Li et al., 1998), K-feldspar $^{40}Ar/^{39}Ar$ ages (Cheilletz et al., 2010), zircon U-Pb dating (Zhu et al., 2006), thermally activated electron spin resonance (ESR) dating for quartz (Zou et al., 2016), and K-Ar dating for micas or whole rocks (Zhang, 1995; Wang et al., 2014). In this study, we have applied an integrated approach to determine the mineralization age of fluorite deposits using the data collected from previous studies. The approaches that were applied are as follows: (1) A consistent result from multiple dating methods is preferred. For instance, the Huangshaping deposit displays a consistent dating result from Re-Os isochron for coexisting molybdenite (~155.3 to 162.7 Ma) and U-Pb ages for zircon (152 ± 3 Ma) (Lei et al., 2010; Zhu et al., 2012). (2) We favored direct dating results to indirect ones when they are not mutually consistent. For instance, the Yutoushan deposit in Zhejiang was determined to form at 81.70 to 87.75 Ma through fluorite fission-track dating and 85 ± 3.5 Ma by fluorite Sm-Nd isochron dating; however, the zircon and mica in the hosted granitic and volcanic rocks determine the U-Pb age of 100.3 ± 0.6 Ma and Ar-Ar age of 160.82 ± 1.68 Ma, respectively (Zhang, 1995; Liu et al., 2014; Wang et al., 2014). In this case, the direct dating results are consistent with the mineralization ages of fluorite deposits nearby, including a fluorite Sm-Nd age of 90 ± 12 Ma for the Yangjia deposit, a valencianite K-Ar age of 79.5 Ma for the Wuzhai deposit, and a fluorite Sm-Nd age of 85.8 ± 3.8 Ma for the Houshu deposit (Han et al., 1991; Li and Wang, 1996; Wang et al., 2014). Thus, we chose the direct dating result as its mineralization age for the Yutoushan deposit. (3) when

direct fluorite dating was absent we selected dating results from coexisting minerals with fluorite, taking the regional mineralization age into consideration. The Lutang deposit in Zhejiang, for example, has only an indirect dating result of 85.6 Ma determined by K-Ar dating for coexisting biotite (Li and Wang, 1996), which is consistent with the age of regional fluorite mineralization. Therefore this indirect age can be reliably used to determine the hydrothermal activity and mineralization for the Lutang deposit.

Compiled geochronological data, which are provided in Table S1, show that the mineralization ages of the fluorite deposits from southeast China fall mainly into three major epochs: 165–150 Ma (Epoch I), 150–130 Ma (Epoch II), and ~110–70 Ma (Epoch III) (Fig. 2a). Relative to the fluorite deposits, the host or wall rocks that are closely associated with fluorite deposits show older ages (Fig. 2b). The magmatic rocks related to Epoch III fluorite deposits display a broad formation age range between ~140 and 100 Ma, with a peak at 130–120 Ma, which is 20–50 Myrs earlier than those of the Epoch III fluorite deposits. Because most of the Epoch III fluorite deposits existing as a quartz-fluorite association are genetically related to the host felsic intrusive or volcanic rocks (Gu, 2013; Wang et al., 2014; Liu, 2015), they could be formed either at the late magmatic-hydrothermal stage or at the epithermal stage that is unrelated to magma activity, as discussed below in detail. Comparatively, the magmatic rocks associated with the Epoch I and II fluorite deposits show much smaller formation age differences with the corresponding fluorite deposits. This might be because, except for a few vein filling styles, fluorite deposits from Epochs I and II are generally accompanied by other metallic mineralization, typical of magmatic-hydrothermal systems. This implies that fluorite crystallization would mainly happen at the magmatic-hydrothermal stage, slightly later than the zircon crystallization of the magmatic stage.

Spatially, most fluorite deposits formed in the three epochs can be roughly divided into three belts (Fig. 3). Epoch I fluorite deposits are mainly distributed in the Nanling orogen, stretching across ~700 km from the northern Guangxi and southern Hunan provinces into the northern Guangdong and southern Jiangxi provinces. Representative Epoch I fluorite deposits include the Shizhuyuan, Xianghuapu, and Huangshaping deposits (Zhang et al., 2012; Zhu et al., 2012; Wang et al., 2014). Most of these fluorite deposits are accompanied by other metallic mineralization, but a few occur as hydrothermal veins with a quartz-fluorite association. Significantly, most of these deposits constitute a

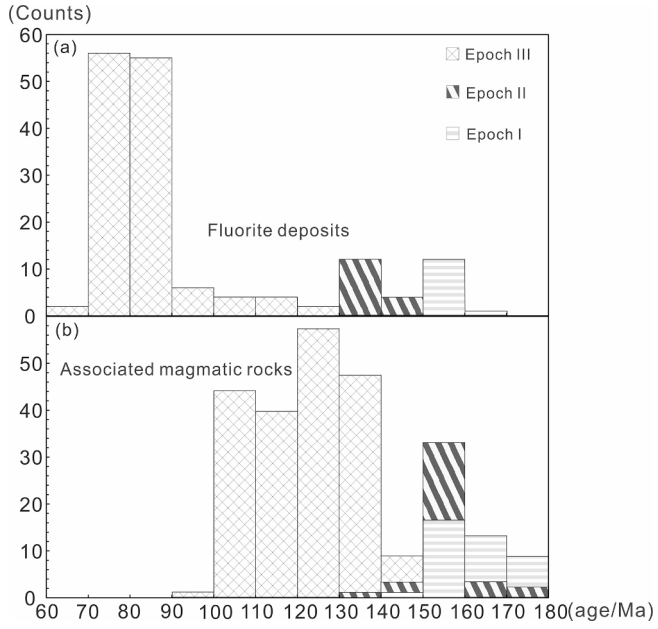

Fig. 2. The age distribution of late-Mesozoic fluorite deposits (a) and associated magmatic rocks (b) in southeast China collected in this study.

middle-Jurassic fluorite deposit belt (FDB), i.e., FDB I. Epoch II fluorite deposits occur mostly in the southeastern Hunan, southeastern Jiangxi, and eastern Fujian provinces, and form a late-Jurassic fluorite deposit belt (FDB II), as represented by the Gaoming, Tangqian, and Chenggang fluorite deposits (Yang, 1989; Xiao, 1992; Hou and Yang, 2016). The FDB II shows a NW-SE orientation, parallell to the FDB I, but is systematically younger (Fig. 3). The mineralization ages of fluorite deposits and the younger trend from the FDB I to II are roughly consistent with those of late-Mesozoic granitoids and W-Sn polymetallic deposits in the same areas (Hu and Zhou, 2012; Sun et al., 2012; Mao et al., 2013). Approximately half of the fluorite deposits in southeast China were formed during Epoch III. These deposits extend for ~1000 km over the southern Zhejiang, western Fujian, eastern Jiangxi, and northeastern Guangdong provinces, with an obvious NE-SW trend, and form a Cretaceous fluorite deposit belt (FDB III; Fig. 3). The Yangjia, Hushan, Houshu, and Bamianshan fluorite deposits are representative (Yuan et al., 1979; Han and Zhang, 1985; Li and Jiang, 1989, 1992; Li and Wang, 1996; Li et al., 1998; Ma et al., 2000; Wang et al., 2014; Ye, 2014). FDB III peaked much later (90–70 Ma) than FDB I and II (Fig. 2a) and is approximately synchronous with the Cu-Mo mineralization belt near the present coast (Zhong et al., 2017; Liu et al., 2018b).

FDB I and II are considerably less exposed and zoned than FDB III. This likely reflects the fact that the older fluorite deposits are not as well preserved due to long-term denudation and alteration. Since the late-Triassic, South China has been dominated mainly by an extensional regime (Zhou et al., 2006; Li and Li, 2007), such that the crust has been largely eroded and massive granitoids that have been emplaced ~10 km below the surface have been exposed. Large-scale, late-Jurassic tectonic activities most likely contributed to the denudation of fluorite deposits in South China. In contrast to the older FDB I and II, the most recent fluorite deposits of FDB III along the coast have undergone less uplift and erosion and are thus better preserved.

4. Discussion

4.1. The origin and concentration processes of fluorine in subduction zones

Given that fluorite comprises CaF_2, calcium is likely derived from common silicate minerals widespread existing in the crust (Zhang, 1995; Wang et al., 2014), the fluorine's origin is thus a key problem for deciphering the genesis of a fluorite deposit. There are three known potential origins for F enrichment in the continental crust. First, fluorine could be transported by F-bearing fluids (e.g., supercritical fluids (SCF), gas, or magmas) into the continental crust from the deep Earth. Lamarre and Hodder (1978) proposed that F can be concentrated in alkalic magmas derived by the partial melting of phlogopite-bearing mantle rocks, and be transported upwards by alkalic magmas and the accompanying vapor phases, such as SiF_4 or HF. Second, magma differentiation can result in a gradual concentration of F in silicate melts (Chen et al., 2018). When F in a highly-evolved melt is sufficiently concentrated, it could be incorporated into the equilibrated magmatic fluids (Carroll and Webster, 1994), forming F-rich fluids with up to 5 wt% F (Bailey, 1977). Finally, F-bearing sedimentary or metamorphic rocks, which either originated from F-rich magmatic parental rocks or were previously altered by F-rich fluids, can supply large amounts of F through the interactions with various high-temperature hydrothermal fluids or low-temperature aqueous fluids, through hydrothermal alteration, weathering, and leaching. In this regard, regional-scale fractures could provide pathways for large-scale water–rock interactions. As a consequence, F-rich igneous provinces in America have been found to correlate well with increased F levels in water supply and the distribution of fluorite deposits (Bailey, 1977). Furthermore, the F-rich basinal brines derived by leaching of shallow, low-temperature aqueous fluids from the associated magmatic rocks also facilitate the formation of Mississippi Valley-type fluorite deposits in Mexico (González-Sánchez

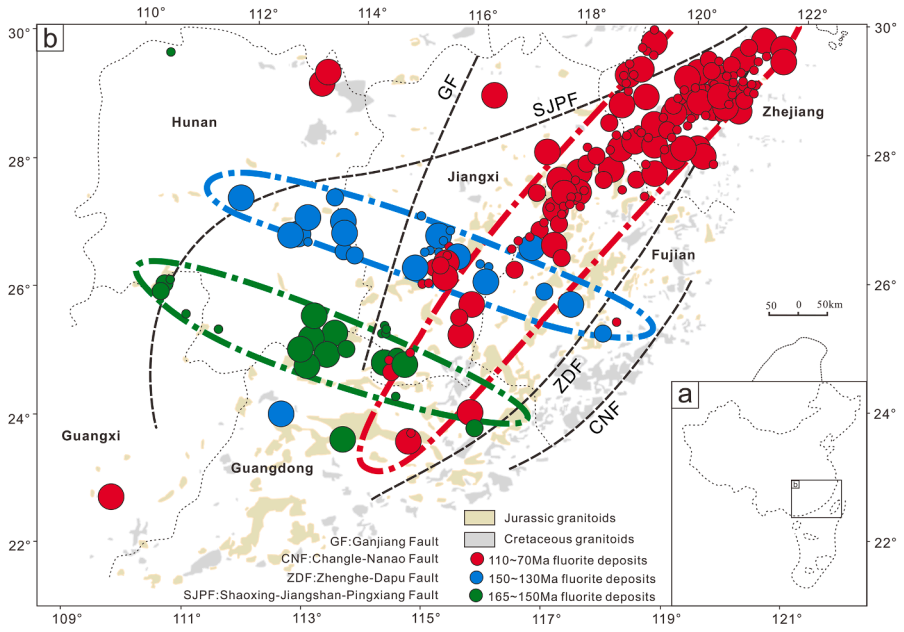

Fig. 3. Sketched maps for (a) southeast China located in the circum-Pacific region, and (b) the temporal and spatial distribution of late-Mesozoic fluorite deposits, as well as granitoids (Zhou et al., 2006), in southeast China. Late-Mesozoic fluorite deposits are not spatially correlated with the four large abyssal faults, and show systematically decreasing ages towards the coast, similar to the granitoids (Zhou et al., 2006), the volcanic rocks (Zhou and Li, 2000), and the metallic ore deposits (Wang et al., 2011; Mao et al., 2013; Zhong et al., 2017; Liu et al., 2018b). Most of them can be divided into three fluorite deposit belts with different mineralization ages and distribution orientation. The largest size of the fluorite deposit spots stand for the largest deposit whose reserve is more than 1 million tons, and the smallest one for the smallest reserve <0.2 million tons, while medium-size spots are in between.

et al., 2009; Camprubí, 2013; González-Partida et al., 2019).

Forearc magmas are usually low in F, and thus most of the F (95%) in the subducting slab is retained in the slab and taken deeper into the mantle during subduction (Straub and Layne, 2003). Fluorine can substitute OH^- and be easily incorporated into OH-bearing minerals (Aoki et al., 1981). Following this rationale, when the subducted slab reaches the eclogite facies, most F is hosted in serpentine, apatite, and particularly in phengite and lawsonite (Philippot et al., 1995; Pagé et al., 2016). Serpentine is unstable at temperatures over 700 °C, and lawsonite decomposes at temperatures between 700 °C and 800 °C, whereas phengite and apatite break down at temperatures between 900 °C and 1300 °C, depending on the pressure (Fig. 4a). As a result, cold plate subduction can cause the decomposition of serpentine and lawsonite, while hot plate subduction or slab rollback can result in the breakdown of all F-bearing minerals, including apatite and phengite (Fig. 4a). In a cold subduction scenario, only at subduction depths up to 300 km would F-bearing minerals break down to generate the F-rich SCF (Fig. 4b). Therefore, some F-rich regions could be located quite distally from a

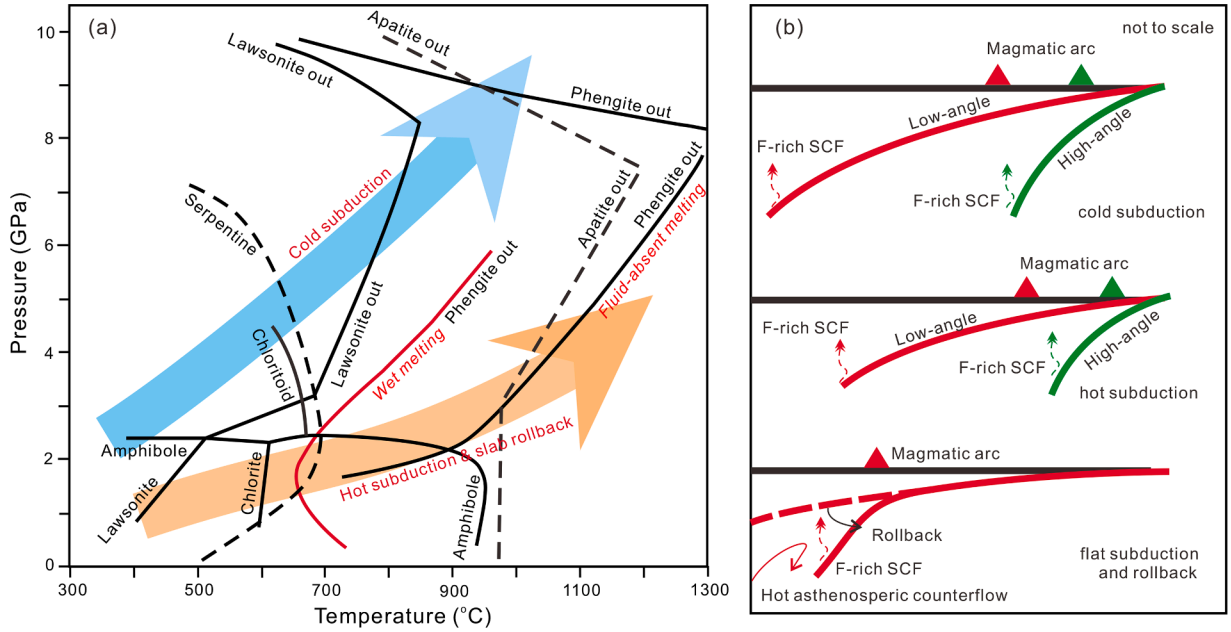

Fig. 4. P-T stability fields for F-bearing minerals (a) and a diagrammatic sketch of different subduction models associated with the release of F-rich fluids and the formation of the magmatic arc (b). (a) The stability fields for amphibole, chlorite, chloritoid, serpentine, phengite and lawsonite are modified from Jiang et al. (2018) and Schmidt and Poli (2014), and the apatite from Konzett et al. (2011). The phengite-out lines with respect to temperature denote the likely location of phengite decomposition in H_2O-saturated systems (MORB) and in fluid-absent systems (pelite), respectively (Schmidt and Poli, 2014). (b) In the cold subduction zone F-bearing mineral dehydration produces F-rich supercritical fluids only at subduction depths of up to 300 km, whereas F-bearing mineral-dominated decomposition likely occurs at shallower depths during hot subduction or slab rollback, allowing for F-rich fluids to be easily generated. During flat-slab subduction in particular, F-rich fluids cannot be released because of low temperature and a too shallow subduction depth. When slab rollback subsequently happens, the surface of the subducted slab is heated up to ~1300 °C by the hot asthenospheric counterflow, resulting in F-bearing mineral decomposition and formation of the F-rich fluids.

given magmatic arc and plate boundary, even in areas of high-angle subduction (Fig. 4b). It is noteworthy that the release of F resulting from serpentine and lawsonite breakdown during cold subduction would be expected to cause a broad crustal dispersion of F as a result of the long distance that F-bearing magmas and SCF would have to cross between the descending slab and upper crust. In such a case, a belt of fluorite deposits would not be easily generated. In contrast, at shallower depths and in association with relatively high-temperature processes, such as hot subduction, as well as flat subduction and the consequent rollback, could easily cause F-bearing minerals to break down, resulting in the F-rich SCF and related magmas (Fig. 4). In these two subduction models, heat-induced dehydration of the subducted slab that involved all F-bearing minerals could easily produce F-rich SCF. Moreover, shallow subduction could facilitate the transport of F from the subducting slab to the crust (Fig. 4b). Therefore, both models of hot subduction and slab rollback could contribute to the massive F flux and the formation of the FDB in subduction zones.

The transport of F from the subducting slab to the overlying crust could have involved a series of complex magmatic and hydrothermal processes. High temperatures associated with hot subduction or slab rollback would cause dehydration of F-bearing minerals in the subducting plate, thus allowing for the subsequent formation of the F-rich SCF (Fig. 5a). The overriding mantle peridotite would be metasomatised by the F-rich SCF resulting in a phlogopite-rich source. Subsequent melting of this source would have generated K- and F-rich alkalic magmas (Lamarre and Hodder, 1978; Zou et al., 2003; Sun et al., 2013; Jiang et al., 2018). The alkalic magma would have either risen up to heat the crust generating calc-alkalic magmas or else evolved into new calc-alkalic and younger F-bearing alkalic magmas (Fig. 5b). During this process, the F-rich hydrothermal fluids would have been differentiated from the evolved calc-alkalic or alkalic magmas (Carroll and Webster, 1994; Chen et al., 2018) and fluxed into the continental crust, accompanied by the upwelling of F-bearing magma, facilitating F transport from the subducted slab to the surface (Fig. 5b). In this regard, subduction-driven magmatism and associated F-rich fluid activities, as well as subsequent metasomatism in the shallow crust could further F cycling and concentration.

In certain circumstances, F-poor fluids might extract and concentrate fluorine by leaching from F-rich wall-rocks. These F-poor fluids might originate from dehydration of the subducting slab not involving F-bearing minerals (e.g., serpentine, apatite, phengite, and lawsonite) (Schmidt and Poli, 2014), from the exsolution of subduction-associated low-F felsic magmas (Anderson, 1989; Chen et al., 2018), or crustal non-magmatic, epigenetic fluid activities along shallow fractures that are controlled by plate subduction (Levresse et al., 2003; Munoz et al., 2005; Camprubí, 2013; Pei et al., 2017; González-Partida et al., 2019). It is evident that concentrating F from F-poor fluids is much difficult than from the F-rich ones, likely resulting in a lower possibility of F mineralization. Moreover, due to the influence of plate subduction, the distribution of these F-poor fluid activities and associated F enrichment would have a linear arrangement parallel to the plate boundary (Anderson, 1989).

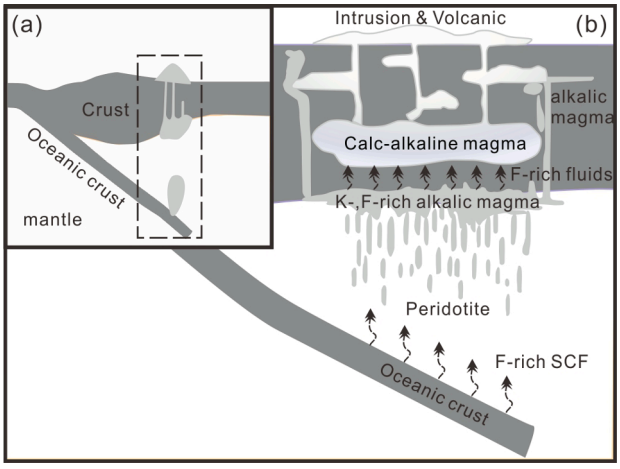

Fig. 5. A revised model for the genesis of subduction-related fluorite deposits (a) and the transport of massive F via F-rich fluids and alkalic magmas (b), modified from Lamarre and Hodder (1978) and Zhou and Li (2000), not to scale.

Fluorine can combine with a great variety of elements to form soluble complexes in the SCF, hydrothermal or aqueous fluids, e.g., CaF_2, Na_2CaF_4, Ca_2Cl_3F, $REEF_3$, SiF_4, $NaAlF_4$, $KBeF_3$, $[AlF_2(H_2O)_4]^+$, $[SiF_6]^{2-}$, $[Sn(OH,F)_6]^{2-}$, $[Ti(OH,F)_6]^{2-}$, $[Zr(OH,F)_6]^{2-}$, $[(Nb,Ta)(OH,F)_7]^{2-}$, etc. (Bailey, 1977; Lamarre and Hodder, 1978; Wang and Chou, 1987; Wang et al., 1993; Williams-Jones et al., 2000; Damdinova and Reyf, 2008; He et al., 2015b, 2015a; Yan et al., 2020). These complexes can migrate upwards in the crust and can hydrolyze to form fluorite and accompanying minerals due to the changes in environmental conditions (Damdinova and Reyf, 2008; Ding et al., 2018) or a reduction in the F activity (Williams-Jones et al., 2000). For example, F-rich fluids that contain F-bearing complexes react with Ca-bearing end members (e.g., carbonate and Ca-bearing fluids), resulting in a reduction of the F activity, and thus the formation of fluorite and accompanying minerals (Lamarre and Hodder, 1978; González-Sánchez et al., 2009). In addition, in the fluids containing CaF_2-bearing complexes (e.g., CaF_2, Na_2CaF_4, Ca_2Cl_3F), CaF_2 solubility or CaF_2-bearing complex's stability will decrease when temperature declines or pH rises (Damdinova and Reyf, 2008; Zhang et al., 2017b). This process can readily cause fluorite deposition.

4.2. The link between formation of the fluorite deposit belts in southeast China and plate subduction

Although a single fluorite deposit can be derived by hydrothermal activity through large-scale fluid circulation, most likely controlled by a series of shallow fractures or faults (Han et al., 1992; Munoz et al., 2005), the three large FDB that extend for over 700 km in southeast China are unlikely to have been formed by such activity. If the rising channel of ore-forming fluids is controlled by large deep faults, the fluorite deposits will distribute along those large deep faults. However, the three large FDB in southeast China are not spatially correlated with large deep faults, e.g., the CNF, the ZDF, the GF, and the SJPF (Fig. 3). Therefore, fault-controlled fluid activity is not the primary cause of FDB in southeast China.

Subduction zones and continental rifts have long been proposed as two first-order tectonic settings responsible for forming the large FDB (Alstine Van, 1976; Lamarre and Hodder, 1978). Since the Mesozoic, tectonic evolution of South China has been successively dominated by the subduction of the Tethys and (paleo-) Pacific plates, suggesting that a continental rift setting is unlikely (Li and Li, 2007; Shu et al., 2009; Dmitrienko et al., 2018; Li et al., 2019). Moreover, as mentioned above, most of the fluorite deposits from the three FDB in southeast China are closely associated with Mesozoic felsic or alkalic magmatic rocks (Lu et al., 2003; Li et al., 2012, 2015; Zhao et al., 2016; Hu et al., 2017). These magmatic rocks have long been considered to be the product of (paleo-) Pacific plate subduction (Zhou and Li, 2000; Zhou et al., 2006; Li and Li, 2007). Massive F fluxes and formation of the FDB in southeast China were most likely associated with plate subduction and related magmatic and hydrothermal processes.

It is known that subducted slab-releasing SCF can lower the solidus curve of rocks in the mantle and the crust to produce more or less linearly shaped magmatic arcs (Anderson, 1989; Tatsumi, 2005). In such a scenario, subduction-derived fluids, i.e., slab-releasing SCF, subduction-related magma-derived hydrothermal fluids, or fault-controlled shallow low-temperature fluids, could easily leach and extract F from the crust to generate a linear FDB along with the contemporaneous magmatic arcs, if the crustal rocks were rich enough in F. However, the FDB in southeast

China do not correlate well in space with subduction-induced volcanic arcs (Fig. 3). FDB I and II are located in an intraplate setting, whereas FDB III occurs mostly in the back-arc except for deposits in central Zhejiang that are situated within the main arc (Fig. 3). This suggests that the formation of most of the FDB in southeast China was genetically associated with subduction-derived F-rich SCF as well as back-arc magmas and exsolved hydrothermal fluids, instead of subduction-derived sub-arc fluids and related arc magmatism. This could also explain the small formation age gaps between the FDB I and II and their associated magmatic rocks (Fig. 2). Furthermore, given the larger and broader age gap (20–50 Myrs) between the deposits of FDB III and the associated magmatic rocks (Fig. 2), some fluorite deposits from FDB III, especially in central Zhejiang, likely originated from the prolonged interaction between the subduction-derived F-poor fluids (e.g., slab-releasing sub-arc SCF, arc magma-derived hydrothermal fluids, fault-controlled shallow low-temperature fluids) and the wall-rocks that fluids have passed through. As discussed above, these F-poor fluids would take longer to concentrate F from the wall-rocks and the formation of fault-controlled shallow low-temperature fluids, would occur much later than the slab-releasing sub-arc fluids and associated arc magma and hydrothermal fluids.

4.3. Subduction style of the (paleo-) Pacific plate in the late Mesozoic

From the perspective of the FDB, southeast China appears to have been dominated by subduction of the (paleo-) Pacific plate since the Jurassic. The FDB III in southeast China displays an obvious NE-SW trend (Fig. 3), suggesting northwestward subduction of the Pacific plate during the Cretaceous. This is consistent with the general consensus about the matter (Zhou and Li, 2000; Zhou et al., 2006; Li and Li, 2007). Since the Mesozoic, southeast China has interacted successively with three (paleo-) Pacific plates, i.e., the Farallon, Izanagi, and Pacific plates (Maruyama et al., 1997; Li et al., 2019). In the early Jurassic, the ridge between the Farallon and the Izanagi plates drifted northwards to North China (Maruyama et al., 1997), whereas the ridge between the Izanagi and Pacific plates possibly reached the position of the Lower Yangtze River in eastern China during the early Cretaceous (Maruyama et al., 1997; Sun et al., 2007), resulting in ridge subduction under the Lower Yangtze River Metallogenic belt (Ling et al., 2009). This implies that in the early Cretaceous, southeast China was likely influenced by northwestward hot subduction of a young and hot Pacific plate. Because the FDB III does not overlap with the Cretaceous volcanic arcs, but both are close to the plate boundary, the subduction angle was probably relatively high (Tatsumi, 1986; Xu et al., 2003; Cao et al., 2011; Arai et al., 2017). Relatively high-angle hot subduction of the Pacific plate could have resulted in sub-arc F-poor fluid activities and volcanic magmatism as well as back-arc F-rich fluid activities and related magmatism. It then triggered the interaction between the shallow low-temperature hydrothermal fluids and F-rich wall-rocks, coupled with subsequent back-arc F-rich fluid release and magmatism (Fig. 5a). Therefore, northwestward high-angle subduction of the Pacific plate would likely explain the FDB III distribution and its spatial association with the Cretaceous magmatic arc in southeast China (Fig. 6).

In contrast, the NW-SE trend distribution of FDB I and II suggest that southeast China was not dominated by the northwestward subduction of (paleo-) Pacific plate before the Cretaceous. Instead, their formation can be explained by rollback of the (paleo-) Pacific plate or northeastward subduction of the Neo-Tethys plate. There are two major reasons to rule out Neo-Tethys subduction. Firstly, the suture zone of the Neo-Tethys plate subduction is believed to be located southwest of Baoshan-Sibumasu and the South China Sea (Royden et al., 2008; Seton et al., 2012; Metcalfe, 2013), which is far away from the Nanling orogen. Although Zhang et al. (2017a) has proposed that Neo-Tethys ridge subduction led to the formation of Shilu adakitic rocks and Cu-Mo mineralization in southern Guangdong, the influence of Neo-Tethys subduction has not been documented to spread to the northern

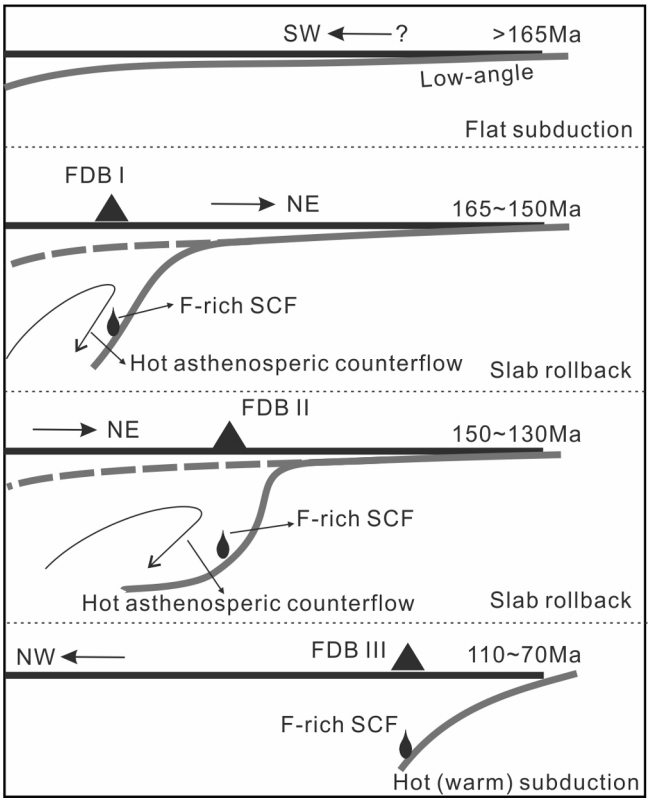

Fig. 6. Sketch maps showing the genesis of three fluorite deposit belts in southeast China and changes in the subduction style of the (paleo-) Pacific plate in the late Mesozoic, not to scale. The slab rollback experienced two stages. The first slab rollback commenced at ~165 Ma, with the hinge near the FDB I. The second slab rollback started at ~150 Ma, forming the FDB II.

Guangdong region, or even to the Nanling orogen. Secondly, the northeastward subduction of the Neo-Tethys plate cannot explain why the formation age of the FDB II is younger than that of the FDB I, although the subduction and subsequent northeastward rollback of the (paleo-) Pacific plate could explain this.

A model of flat-slab subduction and subsequent rollback could reasonably explain the temporal-spatial distribution of the FDB I and II (Fig. 6). The subduction of the (paleo-) Pacific plate would have initiated as very low angle subduction during the Jurassic. The subducted slab could extend to the Nanling orogen, and be followed by northeastward slab rollback in the mid-Jurassic (Li et al., 2012; Zeng et al., 2016). During slab rollback, the subducted slab would have been heated up dramatically by the counterflow of the asthenospheric mantle. This, in turn, would have caused the breakdown of all F-bearing minerals, thus releasing F-rich SCF. Most of these fluids would have been channelized upwards near the hinge of the slab due to the opening of space and counterflow triggered by slab rollback (Fig. 6). Partial melting of mantle rocks altered by the F-rich SCF could have produced alkalic magmas (Lamarre and Hodder, 1978). Fluorine was thus transported into the crust via F-rich SCF and alkalic magmas (Fig. 5b). The presence of F in the magma can significantly lower the solidus temperature of a granitic magma allowing for the formation of the highly-evolved F-rich granites widely distributed throughout southeast China. We propose that slab rollback experienced two stages, with two hinges as illustrated in Fig. 6. The first slab rollback would have commenced at ~165 Ma, with the hinge located across the Nanling region, forming FDB I. A second slab rollback would have then followed at ~150 Ma. This resulted in the formation of the FDB II, which is roughly parallel to the FDB I (Fig. 3b).

4.4. Transition of subduction of the (paleo-) Pacific plate

As discussed above, the high-angle northwestward hot subduction of the Pacific plate could have contributed to the formation of the FDB III. In contrast, the possible possibleflat-slab subduction and subsequent northeastward rollback of the (paleo-) Pacific plate would have been responsible for forming the FDB I and II. However, this raises the question: how did one subduction style shift into the other during the early Cretaceous?

The potential change in the subduction direction of the (paleo-) Pacific plate beneath the Eurasian continent is consistent with the drifting history of the Pacific plate (Fig. 7). Based on island chain ages in the Pacific Ocean, Sun et al. (2007) proposed an abrupt change from southwestward to northwestward in the drifting direction of the Pacific plate at 120–125 Ma. This resulted in a significant tectonic shift in eastern China from extension to transpression, which induced a series of magmatic and gold metallogenic events. If the distribution of three fluorite deposit belts were indeed controlled by the subduction of the Pacific plate, it is very likely that their arrangement reflects a major change in the subduction direction of the subducted Pacific plate during the early Cretaceous. Significantly, two-stage slab rollback in the late Jurassic would have caused high-angle subduction (Fig. 6). Given the low viscosity on the hinge of a high angle rolling slab or imbalance-rollback induced slab tear (Stegman et al., 2006), slab breakoff ultimately occurred (Zeng et al., 2016; Li et al., 2019), which would have reduced the slab pull. This would have resulted in a re-adjustment of the subduction style and/or facilitation of subduction direction change driven by external forces. It has been proposed that the eruption of the Ontong Java large igneous province in the northwestern Pacific Ocean may have played a crucial role in the change of the drift direction of the Pacific plate by ~80° from southwestward to northwestward at ~120–125 Ma (Sun et al., 2007).

Alternatively, the disparate subduction styles that occurred during the late Mesozoic could stem from two different (paleo-) Pacific plates. The Izanagi plate and the Pacific plate interacted successively with southeast China in the Mesozoic (Maruyama et al., 1997; Ling et al., 2009; Li et al., 2019). Although the drifting route of the Izanagi plate and the exact time of interaction with southeast China have not been well defined, the tectonic evolution of southeast China was likely controlled by the Izanagi plate subduction in the late Jurassic, and by the Pacific plate subduction in the Cretaceous (Sun et al., 2007; Li et al., 2013). It is possible that FDB I and II in southeast China were derived from the subduction and northeastward rollback of the Izanagi plate, and that the FDB III was derived by the northwestward subduction of the Pacific plate. The northward movement of the spreading ridge between the Izanagi and Pacific plates (Maruyama et al., 1997), as well as the eruption of the Ontong Java large igneous province (Sun et al., 2007), would have facilitated the transition of subduction in the late Mesozoic.

No matter the type of oceanic plate subduction, the formation of the three FDB and their spatial and temporal distribution tells us that the plate subduction processes were complicated, and most likely accompanied by changes in subduction style, such as subduction direction, angle, and kinetic process. This is particularly useful in reconstructing the evolution of some oceanic or continental plates and examining the precise processes behind plate subduction.

5. Conclusions

Three late-Mesozoic fluorite deposit belts with distinct ages and orientations can be distinguished in southeast China. The FDB I is distributed in the northern Guangxi, the northern Guangdong, and the southern Jiangxi provinces, and formed at ~165–150 Ma. The FDB II extends from the central Hunan to the central Jiangxi province and toward the coast, and formed ~20 Ma later than FDB I. Both the FDB I and II show a NW-SE trend. The FDB III displays a NE-SW trend from the central Zhejiang to the western Fujian and the eastern Guangdong provinces, and it spans the youngest ages (110–70 Ma).

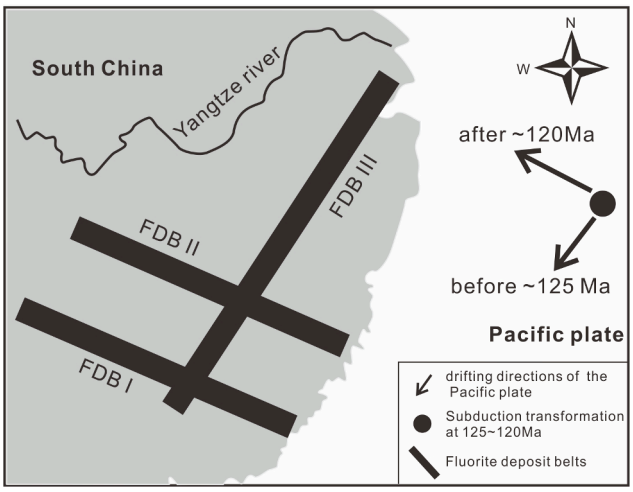

Fig. 7. A sketch map showing that the temporal and spatial distributions of the three fluorite deposit belts in southeast China are reasonably compatible with the changes in the drifting directions of the Pacific plate from SW to NW at 125–120 Ma (Sun et al., 2007), not to scale.

Most of the three FDB are closely associated with Mesozoic felsic and alkalic magmatic rocks derived by the subduction of (paleo-) Pacific plate. We propose that F derived from the decomposition of high-pressure minerals (e.g., phengite, apatite) was transported from the subducted slab and mantle wedge to the surface in F-rich superficial fluids (SCF) and alkaline magmas during the subduction of the (paleo-) Pacific plate. Northeastward slab rollback during low-angle subduction of the (paleo-) Pacific plate during the middle and late-Jurassic led to the formation of the FDB I and II. During this process, slab-releasing F-rich SCF and mantle-derived alkaline magmas, as well as subsequent back-arc magmas and associated high-temperature hydrothermal fluids, played a dominant role on the formation of the FDB I and II. In contrast, FDB III is inferred to be derived by the relatively high-angle northwestward hot subduction of the Pacific plate during the Cretaceous. The formation of the FDB III would be, therefore, involved in two major processes, i.e., back-arc slab-releasing F-rich SCF and consequent magmatic-hydrothermal fluid activities, and the sub-arc slab-releasing F-poor fluids and fault-controlled shallow low-temperature fluid activities. Therefore, heat-induced dehydration of the subducted slab that involved all possible F-bearing minerals would most likely contribute more effectively to the formation of the FDB.

Declaration of Competing Interest

The authors declare the following financial interests/personal relationships which may be considered as potential competing interests: Xing Ding: Guangzhou Institute of Geochemistry, CAS, China. Wei-dong Sun: Institute of Oceanology, CAS, China. On behalf of all co-authors.

Acknowledgments

We thank the two anonymous reviewers and Prof. Pete Hollings for their constructive comments and suggestions. X.D. was supported by the National Key R&D Program of China (2016YFC0600204), the Strategic Priority Research Program of the Chinese Academy of Sciences (XDB42000000) and the Guangdong Major Project of Basic and Applied Basic Research (Grant No. 2019B030302013). W.D.S. was supported by the National Key R&D Program of China (2016YFC0600408), the Taishan Scholar Program of Shandong (ts201712075) and the AoShan Talents Cultivation Program Supported by Qingdao National Laboratory for Marine Science and Technology (2017ASTCP-OS07). This is

contribution No. IS-2940 from GIGCAS. Figs. 2 and 3 in this paper are derived from the data of Table S1, which is stored in the Dryad (doi:10.5061/dryad.wstqjq2gk).

Appendix A. Supplementary data

Supplementary data to this article can be found online at https://doi.org/10.1016/j.oregeorev.2020.103865.

References

Alstine Van, R.E., 1976. Continental rifts and lineaments associated with major fluorspar districts. Economic Geology 71, 977-87. 10.2113/gsecongeo.71.6.977..

Anderson, D.L., 1989. Theory of the Earth. Blackwell scientific publications, Boston, pp. 1–366.

Aoki, K., Ishiwaka, K., Kanisawa, S., 1981. Fluorine geochemistry of basaltic rocks from continental and oceanic regions and petrogenetic application. Contrib. Mineral Petrol. 76 (1), 53–59. https://doi.org/10.1007/BF00373683.

Arai, R., Kodaira, S., Yamada, T., Takahashi, T., Miura, S., Kaneda, Y., Nishizawa, A., Oikawa, M., 2017. Subduction of thick oceanic plateau and high-angle normal-fault earthquakes intersecting the slab: seamount and Normal-Fault Earthquakes. Geophys. Res. Lett. 44 (12), 6109–6115.

Bailey, J.C., 1977. Fluorine in granitic rocks and melts: a review. Chem. Geol. 19 (1-4), 1–42. https://doi.org/10.1016/0009-2541(77)90002-X.

Camprubí, A., 2013. Tectonic and metallogenic history of Mexico. Society of Economic Geologists Special Publication 17, 201–243.

Cao, J.C., 1987. Classification and metallogenic regular of Chinese fluorite deposit. Geol. Explor. 14–19 (in Chinese with English abstract).

Cao, J.C., 1995. REE geochemical characteristics of epithermal vein fluorite deposits in South China. Geochimica 24, 225–234. https://doi.org/10.19700/j.0379-1726.1995.03.003 (in Chinese with English abstract).

Cao, M.J., Qin, K.Z., Li, J.L., 2011. Research progress on the flat subduction and its metallogenic effect, two cases analysis and some prospects. Acta Petrol. Sin. 27, 3727–3748 (in Chinese with English abstract). 1000–0569 /2011 /027(12)-3727-48.

Carroll, M.R., Webster, J.D., 1994. Solubilities of sulphur, noblegases, notrogen, chlorine, and fluorine in magmas. Rev. Mineral. 30, 231–279.

Cheilletz, A., Gasquet, D., Filali, F., Archibald, D.A., Nespolo, M., 2010. A late Triassic 40Ar/39Ar age for the El Hammam high-REE fluorite deposit (Morocco): mineralization related to the Central Atlantic Magmatic Province? Miner. Depos. 45, 323–329. https://doi.org/10.1007/s00126-010-0282-y.

Chen, C., Ding, X., Li, R., Zhang, W.Q., Ouyang, D.J., Yang, L., Sun, W.D., 2018. Crystal fractionation of granitic magma during its non-transport processes: a physics-based perspective. Sci. China Earth Sci. 61, 190–204. https://doi.org/10.1007/s11430-016-9120-y.

Chen, G., Qiu, X.Y., 2013. Review of geological characteristics and genesis of fluorite deposit in China. China Non-Metallic Mining Industry, 47-52(in Chinese with English abstarct). 10.3969/j.issn.1007-9386.2013.05.016.

Chen, J.F., Zhou, T.X., Yin, C.S., 1991. Determination of Ar- (40)Ar- (39)Ar age of some Mesozoic intrusive rocks in southeast zhejiang. Acta Petrologica Sinica, 37-44(in Chinese with English abstract). 10.1007/BF02919155.

Chen, L., Zheng, Y.F., Zhao, Z.F., 2016a. Geochemical constraints on the origin of Late Mesozoic andesites from the Ningwu basin in the Middle-Lower Yangtze Valley, South China. Lithos 254, 94–117. https://doi.org/10.1016/j.lithos.2016.03.012.

Chen, Y.X., Li, H., Sun, W.D., Ireland, T., Tian, X.F., Hu, Y.B., Yang, W.B., Chen, C., Xu, D. R., 2016b. Generation of late meosozic qianlishan A 2 -type granite in nanling Range, South China: implications for shizhuyuan W-Sn mineralization and tectonic evolution. Lithos 266, 435–452. https://doi.org/10.1016/j.lithos.2016.10.010.

Chesley, J.T., Liu, J.S., 1992. The Sm-Nd direct dating of fluorite mineralization. Journal of Geoscience Translations 9, 1-4(in Chinese). 10.15964/j.cnki.027jgg.1992.01.001.

Damdinova, L.B., Reyf, F.G., 2008. The origin of low-Be quartz-fluorite field at the ermakovskoe high-grade F-Be-ore deposit. Russ. Geol. Geophys. 49, 816–826. https://doi.org/10.1016/j.rgg.2008.03.004.

Deng, X.H., Chen, Y.J., Bagas, L., Zhou, H.Y., Yao, J.M., Zheng, Z., Wang, P., 2015. Isotope (S–Sr–Nd–Pb) constraints on the genesis of the ca. 850Ma Tumen Mo–F deposit in the Qinling Orogen, China. Precambr. Res. 266, 108–118. https://doi.org/10.1016/j.precamres.2015.05.019.

Ding, X., Harlov, D.E., Chen, B., Sun, W.D., 2018. Fluids, metals, and mineral/ore deposits. Geofluids 2018, 1–6. https://doi.org/10.1155/2018/1452409.

Ding, X., Sun, W.D., Chen, W.F., Chen, P.R., Sun, T., Sun, S.J., Lin, C.T., Chen, F.K., 2015. Multiple Mesozoic magma processes formed the 240–185 Ma composite Weishan pluton, South China: evidence from geochronology, geochemistry, and Sr-Nd isotopes. Int. Geol. Rev. 57, 1189–1217. https://doi.org/10.1080/00206814.2014.905997.

Dmitrienko, L.V., Wang, P.C., Li, S.Z., Cao, X.Z., Somerville, L., Zhou, Z.Z., Hu, M.Y., Suo, Y.H., Guo, L.L., Y.M., W., X.Y., L., Liu, X., Yu, S.Y., Zhu, J.J., 2018. Meso-Cenozoic Evolution of Earth Surface System under the East Asian Tectonic Superconvergence. Acta Geologica Sinica 92, 814-49. 10.1111/1755-6724.13556.

Doglioni, C., Carminati, E., Cuffaro, M., Scrocca, D., 2007. Subduction kinematics and dynamic constraints. Earth Sci. Rev. 83, 125–175. https://doi.org/10.1016/j.earscirev.2007.04.001.

Fang, Y., Zou, H., Bagas, L., Said, N., Li, Y., Liu, H., 2020. Fluorite deposits in the Zhejiang Province, southeast China: the possible role of extension during the late stages in the subduction of the Paleo-Pacific oceanic plate, as indicated by the Gudongkeng fluorite deposit. Ore Geol. Rev. 117, 103276 https://doi.org/10.1016/j.oregeorev.2019.103276.

Gilder, S.A., Keller, G.R., Luo, M., Goodell, P.C., 1991. Eastern Asia and the Western Pacific timing and spatial distribution of rifting in China. Tectonophysics 197, 225–243. https://doi.org/10.1016/0040-1951(91)90043-R.

González-Partida, E., Camprubí, A., Carrillo-Chávez, A., Díaz-Carreo, E.H., Vázquez-Ramírez, J.T., 2019. Giant fluorite mineralization in central mexico by means of exceptionally low salinity fluids: an unusual style among MVT deposits. Minerals 9, 35. https://doi.org/10.3390/min9010035.

González-Sánchez, F., Camprubí, A., González-Partida, E., Puente-Solís, R., Canet, C., Centeno-García, E., Atudorei, V., 2009. Regional stratigraphy and distribution of epigenetic stratabound celestine, fluorite, barite and Pb–Zn deposits in the MVT province of northeastern Mexico. Miner. Depos. 44, 343. https://doi.org/10.1007/s00126-008-0212-4.

Graupner, T., Mühlbach, C., Schwarz-Schampera, U., Henjes-Kunst, F., Melcher, F., Terblanche, H., 2015. Mineralogy of high-field-strength elements (Y, Nb, REE) in the world-class Vergenoeg fluorite deposit, South Africa. Ore Geol. Rev. 64, 583–601. https://doi.org/10.1016/j.oregeorev.2014.02.012.

Gu, L.F., 2013. The research of metallogenic characteristics and mechanism in Gaowushan fluorite deposite, Zhejiang. Chinese Unversity of Geoscience(Beijing), Beijing, pp. 1-47.

Han, W.B., Ma, C.A., Wang, Y.R., 1991. Geological and Geochemistrial Characteristics of Fluorite Deposit-Take Wuyi Ore Field in Zhejiang Province as An Example. Geology Press, Beijing, pp. 82–92.

Han, W.B., Zhang, W.Y., 1985. The genetic relation between fluorite deposits and subvolcanic rock in Wuyi-Dongyang region. Geol. Zhejiang 1, 28–36 (in Chinese with English abstract).

Han, W.B., Zhang, Y.T., Huang, W.M., Ma, C.A., Wang, Y.R., 1992. Isotope geochemistry of fluorite deposit in Wuyi ore field, Zhejiang Province. Geochemica 354–365 (in Chinese with Englisn abstract).

Han, Y.C., Xia, X.H., Pang, S.Y., Xu, S.K., 2012. Hydrothermal sedimentary mineralization of the super-large Bamianshan fluorite deposit in Zhejiang province, China. Acta Geol. Sin. 86, 762–768.

He, J.J., Ding, X., Wang, Y.R., Sun, W.D., 2015a. The effect of temperature and concentration on hydrolysis of fluorine-rich titanium complexes in hydrothermal fluids: Constraints on titanium mobility in deep geological processes. Acta Petrol. Sin. 31, 802–810 (in Chinese with English abstract).

He, J.J., Ding, X., Wang, Y.R., Sun, W.D., 2015b. The effects of precipitation-aging-re-dissolution and pressure on hydrolysis of fluorine-rich titanium complexes in hydrothermal fluids and its geological implications. Acta Petrol. Sin. 31, 1870–1878 (in Chinese with English abstract).

Hong, D., Niu, Y.L., Xiao, Y.Y., Sun, P., Kong, J.J., Guo, P.Y., Shao, F.L., Wang, X.H., Duan, M., Xue, Q.Q., Gong, H.M., Chen, S., 2018. Origin of the Jurassic-Cretaceous intraplate granitoids in Eastern China as a consequence of paleo-Pacific plate subduction. Lithos 322, 405–419. https://doi.org/10.1016/j.lithos.2018.10.027.

Hou, S.S., Yang, R., 2016. The geological characteristics and genesis of fluorite deposits in Xingguo, Jiangxi Province. Geol. Chem. Miner. 38, 136–143 (in Chinese with English abstract).

Hu, Q.H., Yu, K.Z., Liu, Y.S., Hu, Z.C., Zong, K.Q., 2017. The 131–134 Ma A-type granites from northern Zhejiang Province, South China: implications for partial melting of the Neoproterozoic lower crust. Lithos 294, 39–52. https://doi.org/10.1016/j.lithos.2017.09.016.

Hu, R.Z., Zhou, M.F., 2012. Multiple Mesozoic mineralization events in South China—an introduction to the thematic issue. Miner. Depos. 47, 579–588. https://doi.org/10.1007/s00126-012-0431-6.

Huang, Z.L., Xu, C., Andrew, M., Liu, C.Q., Wu, J., Xu, D.R., 2007. REE geochemistry of fluorite from the maoniuping REE Deposit, Sichuan Province, China: implications for the source of ore-forming fluids. Acta Geol. Sin. 81, 622–636. https://doi.org/10.1111/j.1755-6724.2007.tb00986.x.

Jiang, X.Y., Li, H., Ding, X., Wu, K., Guo, J., Liu, J., Sun, W., 2018. Formation of A-type granites in the Lower Yangtze River Belt: a perspective from apatite geochemistry. Lithos 304–307, 125–134. https://doi.org/10.1016/j.lithos.2018.02.005.

Konzett, J., Rhede, D., Frost, D.J., 2011. The high PT stability of apatite and Cl partitioning between apatite and hydrous potassic phases in peridotite: an experimental study to 19 GPa with implications for the transport of P, Cl and K in the upper mantle. Contrib. Miner. Petrol. 163, 277–296. https://doi.org/10.1007/s00410-011-0672-x.

Lamarre, A.L., Hodder, R.W., 1978. Distribution and genesis of fluorite deposits in the Western United States and their significance to metallogeny. Geology 6, 236–238. https://doi.org/10.1130/0091-7613(1978)6<236:DAGOFD>2.0.CO;2.

Lei, Z.H., Chen, F.W., Chen, Z.H., Xu, Y.M., Gong, S.Q., Li, H.J., Mei, Y.P., Qu, W.J., Wang, D.H., 2010. The age determination and geological significance of metallogenic mineralization in huangshingping lead and zinc polymetallic deposit. Acta Geosci. Sin. 31, 532–540 (in Chinese with English abstract).

Levresse, G., Gonzalez-Partida, E., Tritlla, J., Camprubí, A., Morales-Puente, P., 2003. Fluid characteristics of the world-class, carbonate-hosted Las Cuevas fluorite deposit (San Luis Potosí, Mexico). J. Geochem. Explor. 78, 537–543. https://doi.org/10.1016/S0375-6742(03)00145-6.

Li, C.J., Jiang, X.L., 1989. Fission track dating of fluorite deposit in Zhejiang Province and some related problems. Geochemica. https://doi.org/10.1007/BF02005959, 181–8 (in Chinese with English abstract).

Li, C.J., Jiang, X.L., 1992. Minerogenetic model for two types of fluorite deposits in Southeastern China. Acta Geol. Sin. Engl. Edn. 5, 75–88. https://doi.org/10.1111/j.1755-6724.1992.mp5001005.x.

Li, C.J., Wang, G.W., 1996. Isotopic geochemistry of chinese fluorite deposits. Int. Geol. Rev. 38, 1054–1067. https://doi.org/10.1080/00206819709465381.

Li, C.J., Xu, Y.L., Jiang, X.L., 1998. Neodymium and strontium isotope geochemistry of Wuyi-Dongyang fluorite deposits, Zhejiang Province, Southeast China. Quadrennial Iagod Symposium. p. 258-68.
Li, C.Y., Zhang, H., Wang, F.Y., Liu, J.Q., Sun, Y.L., Hao, X.L., Li, Y.L., Sun, W.D., 2012. The formation of the Dabaoshan porphyry molybdenum deposit induced by slab rollback. Lithos 150, 101–110. https://doi.org/10.1016/j.lithos.2012.04.001.
Li, P.J., Yu, X.Q., Li, H.Y., Qiu, J.T., Zhou, X., 2013. Jurassic-Cretaceous tectonic evolution of Southeast China: geochronological and geochemical constraints of Yanshanian granitoids. Int. Geol. Rev. 55, 1202–1219. https://doi.org/10.1080/00206814.2013.771952.
Li, S., Suo, Y., Li, X., Li, X.Y., Zhou, J., Santosh, M., Wang, P.C., Wang, G.Z., Guo, L.L., Yu, S.Y., Lan, H.Y., Dai, L.M., Zhou, Z.Z., X.Z., C., Zhu, J.J., Liu, B., Jiang, S.H., G., W., Zhang, G.W., 2019. Mesozoic tectono-magmatic response in the East Asian ocean-continent connection zone to subduction of the Paleo-Pacific Plate. Earth-Science Reviews 192, 91-137. 10.1016/j.earscirev.2019.03.003.
Li, X.H., Chen, Z.G., Liu, D.Y., Li, W.X., 2003. Jurassic Gabbro-granite-syenite suites from southern jiangxi province, se china: age, origin, and tectonic significance. Int. Geol. Rev. 45, 898–921. https://doi.org/10.2747/0020-6814.45.10.898.
Li, Y., Hu, Y.H., Wang, J.E., Liu, Y.D., Wang, Z., 2015. Zircon Shrimp U-pb Age of Niutoushan Pluton in Southern Zhejiang and Its Geological Implications. Bulletin of Science and Technology 31, 57-61(in Chinese with English abstract). 10.3969/j.issn.1001-7119.2015.11.012.
Li, Z.X., Li, X.H., 2007. Formation of the 1300-km-wide intracontinental orogen and postorogenic magmatic province in Mesozoic South China: A flat-slab subduction model. Geology 35, 179–182. https://doi.org/10.1130/G23193a.1.
Ling, H.F., Shen, W.Z., Huang, X.L., 1999. Characteristics and significance of nd-sr isotopes in granite of fujian province Acta Petrologica Sinica 15, 255-62(in Chinese with English abstract). 10.3321/j.issn:1000-0569.1999.02.011.
Ling, M.X., Wang, F.Y., Ding, X., Hu, Y.H., Zhou, J.B., Zartman, R.E., Yang, X.Y., Sun, W.D., 2009. Cretaceous Ridge Subduction Along the Lower Yangtze River Belt, Eastern China. Econ. Geol. 104, 303–321. https://doi.org/10.2113/gsecongeo.104.2.303.
Liu, D.R., 2015. Geological characteristics and metallogenic model of "Changshan type" fluorite deposits. Acta Petrol. Et Minral. 34, 343–352 (in Chinese with English abstract).
Liu, D.R., Yan, S.X., Chen, Y., Wang, M.H., Zheng, D., 2012. Geochemical characteristics of the Yanqian high-F granite and its relationship with the new-type Bamianshan fluorite deposit in Northwest Zhejiang Province. Geol. Explor. 48, 884–893 (in Chinese with English abstract).
Liu, H., Sun, W.D., Zartman, R., Tang, M., 2019a. Continuous plate subduction marked by the rise of alkali magmatism 2.1 billion years ago. Nat. Commun. 10, 1–8. https://doi.org/10.1038/s41467-019-11329-z.
Liu, L., Hu, R.Z., Zhong, H., Tang, Y.W., Yang, J.H., Li, Z., Zhao, L., Shen, N.P., 2018a. New constraints on the Cretaceous geodynamics of paleo-Pacific plate subduction: Insights from the Xiaojiang-Beizhang granitoids, Zhejiang Province, Southeast China. Lithos 314–315, 382–399. https://doi.org/10.1016/j.lithos.2018.06.020.
Liu, L., Qiu, J.S., Zhao, J.L., Yang, Z.L., 2014. Geochronological, geochemical, and Sr–Nd–Hf isotopic characteristics of Cretaceous monzonitic plutons in western Zhejiang Province, Southeast China: New insights into the petrogenesis of intermediate rocks. Lithos 196, 242–260. https://doi.org/10.1016/j.lithos.2014.03.010.
Liu, P., Mao, J.W., Santosh, M., Bao, Z.A., Zeng, X.J., Jia, L.H., 2018b. Geochronology and petrogenesis of the Early Cretaceous A-type granite from the Feie'shan W-Sn deposit in the eastern Guangdong Province, SE China: implications for W-Sn mineralization and geodynamic setting. Lithos 300, 330–347. https://doi.org/10.1016/j.lithos.2017.12.015.
Liu, W.H., Jiang, M.R., Xia, Y., Zhou, L., 2019b. Subduction and rollback of the paleo-Pacific plate during the Early Cretaceous: insights from the Jiangmiao gabbroic intrusion in the Lower Yangtze River Belt, central-eastern China. Lithos 330, 211–222. https://doi.org/10.1016/j.lithos.2019.02.018.
Lu, H.Z., Liu, Y.M., Wang, C.L., Xu, Y.Z., Li, H.Q., 2003. Mineralization and fluid inclusion study of the Shizhuyuan W-Sn-Bi-Mo-F skarn deposit, Hunan province, China. Econ. Geol. 98, 955–974. https://doi.org/10.2113/gsecongeo.98.5.955.
Ma, T.H., Zhu, X.S., Li, C.J., 2000. Spatial distribution of fluorite deposit in Zhejiang Province. Mineral Deposit 19, 281-8(in Chinese with English abstract). 10. 16111 /j . 0258 -7106. 2000. 03. 011.
Mao, J.W., Cheng, Y.B., Chen, M.H., Pirajno, F., 2013. Major types and time-space distribution of Mesozoic ore deposits in South China and their geodynamic settings. Miner. Depos. 48, 267–294. https://doi.org/10.1007/s00126-012-0446-z.
Mao, J.W., Zhang, Z.C., Zhang, Z.C., Du, A.D., 1999. Re-Os isotopic dating of molybdenites in the Xiaoliugou W (Mo) deposit in the northern Qilian mountains and its geological significance. Geochim. Cosmochim. Acta 63, 1815–1818. https://doi.org/10.1016/S0016-7037(99)00165-9Get.
Maruéjol, P., Cuney, M., Turpin, L., 1990. Magmatic and hydrothermal REE fractionation in the Xihuashan granites (SE China). Contrib. Miner. Petrol. 104, 668–680. https://doi.org/10.1007/BF01167286.
Maruyama, S., Isozaki, Y., Kimura, G., Terabayashi, M., 1997. Paleogeographic maps of the Japanese Islands: Plate tectonic synthesis from 750 Ma to the present. Isl. Arc 6, 121–142. https://doi.org/10.1111/j.1440-1738.1997.tb00043.x.
Metcalfe, I., 2013. Gondwana dispersion and Asian accretion: tectonic and palaeogeographic evolution of eastern Tethys. J. Asian Earth Sci. 66, 1–33. https://doi.org/10.1016/j.jseaes.2012.12.020.
Munoz, M., Premo, W.R., Courjault-Radé, P., 2005. Sm–Nd dating of fluorite from the worldclass Montroc fluorite deposit, southern Massif Central, France. Miner. Depos. 39, 970–975. https://doi.org/10.1007/s00126-004-0453-9.
Pagé, L., Hattori, K., Hoog, J.C.M.D., Okay, A.I., 2016. Halogen (F, Cl, Br, I) behaviour in subducting slabs: A study of lawsonite blueschists in western Turkey. Earth Planet. Sci. Lett. 442, 133–142. https://doi.org/10.1016/j.epsl.2016.02.054.
Pei, Q.M., Zhang, S.T., Santosh, M., Cao, H.W., Zhang, W., Hu, X.K., Wang, L., 2017. Geochronology, geochemistry, fluid inclusion and C, O and Hf isotope compositions of the Shuitou fluorite deposit, Inner Mongolia, China. Ore Geol. Rev. 83, 174–190. https://doi.org/10.1016/j.oregeorev.2016.12.022.
Philippot, P., Chevallier, P., Chopin, C., Dubessy, J., 1995. Fluid composition and evolution in coesite-bearing rocks (Dora-Maira massif, Western Alps): implications for element recycling during subduction. Contrib. Miner. Petrol. 121, 29–44. https://doi.org/10.1007/s004100050088.
Pi, T., Solé, J., Taran, Y., 2005. (U-Th)/He dating of fluorite: application to the La Azul fluorspar deposit in the Taxco mining district, Mexico. Miner. Depos. 39, 976–982. https://doi.org/10.1007/s00126-004-0443-y.
Qiu, J.S., Wang, D.Z., Brent, M.I.A., 1999. Zhejiang the coastal areas of fujian I-type–A-type complex geochemistry and genesis of granite rock mass. Acta Petrol. Sin. 15, 237–246 (in Chinese with English abstract).
Royden, L.H., Burchfiel, B.C., van der Hilst, R.D., 2008. The geological evolution of the Tibetan Plateau. Science 321, 1054–1058. https://doi.org/10.1126/science.1155371.
Schmidt, M.W., Poli, S., 2014. Devolatilization During Subduction. Oxford, Elsevier-Pergamon, pp. 669-701. 10.1016/b978-0-08-095975-7.00321-1.
Seton, M., Muller, R., Zahirovic, S., Gaina, C., Torsvik, T., Shephard, G., Talsma, A., Gurnis, M., Turner, M., Maus, S., 2012. Global continental and ocean basin reconstructions since 200 Ma. Earth Sci. Rev. 113, 212–270. https://doi.org/10.1016/j.earscirev.2012.03.002.
Shu, L.S., Zhou, X.M., Peng, P., Wang, B., Jiang, S.Y., Yu, J.H., Zhao, X.X., 2009. Mesozoic tectonic evolution of the Southeast China Block: new insights from basin analysis. J. Asian Earth Sci. 34, 376–391. https://doi.org/10.1016/j.jseaes.2008.06.004.
Stegman, D.R., Freeman, J., Schellart, W.P., Moresi, L., May, D., 2006. Influence of trench width on subduction hinge retreat rates in 3-D models of slab rollback. Geochem. Geophys. Geosyst. 7, Q03012. https://doi.org/10.1029/2005GC001056.
Stern, R.J., 2004. Subduction initiation: spontaneous and induced. Earth Planet. Sci. Lett. 226, 275–292. https://doi.org/10.1016/j.epsl.2004.08.007.
Straub, S.M., Layne, G.D., 2003. The systematics of chlorine, fluorine, and water in Izu arc front volcanic rocks: implications for volatile recycling in subduction zones. Geochim. Cosmochim. Acta 67, 4179–4203. https://doi.org/10.1016/S0016-7037(03)00307-7.
Strong, D.F., Fryer, B.J., Kerrich, R., 1984. Genesis of the St. Lawrence fluorspar deposits as indicated by fluid inclusion, rare earth element, and isotopic data. Econ. Geol. 79, 1142–1158. https://doi.org/10.2113/gsecongeo.79.5.1142.
Sun, W.D., Ding, X., Hu, Y.H., Li, X.H., 2007. The golden transformation of the Cretaceous plate subduction in the west Pacific. Earth Planet. Sci. Lett. 262, 533–542. https://doi.org/10.1016/j.epsl.2007.08.021.
Sun, W.D., Li, S., Yang, X.Y., Ling, M.X., Ding, X., Duan, L.A., Zhan, M.Z., Zhang, H., Fan, W.M., 2013. Large-scale gold mineralization in eastern China induced by an Early Cretaceous clockwise change in Pacific plate motions. Int. Geol. Rev. 55, 311–321. https://doi.org/10.1080/00206814.2012.698920.
Sun, W.D., Ling, M.X., Yang, X.Y., Fan, W.M., Ding, X., Liang, H.Y., 2010. Ridge subduction and porphyry copper-gold mineralization: an overview. Sci. China-Earth Sci. 53, 475–484. https://doi.org/10.1007/s11430-010-0024-0.
Sun, W.D., Yang, X.Y., Fan, W.M., Wu, F.Y., 2012. Mesozoic large scale magmatism and mineralization in South China: Preface. Lithos 150, 1–5. https://doi.org/10.1016/j.lithos.2012.06.028.
Tatsumi, Y., 1986. Formation of the volcanic front in subduction zones. Geophys. Res. Lett. 13, 717–720. https://doi.org/10.1029/GL013i008p00717.
Tatsumi, Y., 2005. The subduction factory: how it operates in the evolving Earth. GSA today 15, 4-10. 10:1130/1052-5173(2005)015<4:TSFHIO>2.0.CO;2.
USGS Mineral commodity summaries 2019: USGS 2019 10.3133/70202434.
Wang, C.L., Luo, S.W., Xu, Y.Z., Sun, Y.H., Xie, C.G., Zhang, C.M., Xu, W.G., Ren, X.M., 1987. Geology of Shizhuyuan polymetallic deposit. Geol. Publ, House, Beijing.
Wang, F.Y., Ling, M.X., Ding, X., Hu, Y.H., Zhou, J.B., Yang, X.Y., Liang, H.Y., Fan, W.M., Sun, W.D., 2011. Mesozoic large magmatic events and mineralization in SE China: oblique subduction of the Pacific plate. Int. Geol. Rev. 53, 704–726. https://doi.org/10.1080/00206814.2010.503736.
Wang, J.P., Shang, P.Q., Xiong, X.X., 2014. The Metallogenic Regularity of the Fluorites in China. Geological Publishing House, Beijing, pp. 1–165.
Wang, Q., Li, J.W., Jian, P., Zhao, Z.H., Xiong, X.L., Bao, Z.W., Xu, J.F., Li, C.F., Ma, J.L., 2005a. Alkaline syenites in eastern Cathaysia (South China): link to Permian-Triassic transtension. Earth Planet. Sci. Lett. 230, 339–354. https://doi.org/10.1016/j.epsl.2004.11.023.
Wang, Q., Zhao, Z.H., Jian, P., Xiong, X.L., Bao, Z.W., Dai, T.M., Xu, J.F., Ma, J.L., 2005b. Geochronology of Cretaceous A-type granitoids or alkaline intrusive rocks in the hinterland, South China: constraints for late-Mesozoic tectonic evolution. Acta Petrol. Sin. 21, 795–808. https://doi.org/10.1016/j.sedgeo.2005.01.008 (in Chinese with English abstrcat).
Wang, Y.R., Chou, I.M., 1987. Characteristics of hydrolysis of the complex Na2SnF6 in hydrothermal solutions—An experimental study. Chin. J. Geochem. 6, 372–382.
Wang, Y.R., Gu, F., Yuan, Z.Q., 1993. Partitioning and hydrolysis of Nb and Ta and their implications with regard to mineralization. Chin. J. Geochem. 12, 84–91. https://doi.org/10.1007/BF02869048.
Williams-Jones, A.E., Samoson, I.M., Olivo, G.R., 2000. The genesis of hydrothermal fluorite-ree deposits in the gallinas mountains, New Mexico. Econ. Geol. 95, 327–341. https://doi.org/10.2113/gsecongeo.95.2.327.

Xia, X.H., Han, Y.C., Lian, W., Yuan, C.J., Xu, S.K., Yan, F., Liang, Z.M., 2010. Sedimentary genesis feature of Bamianshan unusual large fluorite deposit in Zhejiang Province. Acta Sedimentol. Sin. 28, 1175–1181 (in Chinese with English abstract).

Xiao, Q., 1992. A brief introduction to Gaoming fluorite deposit. Anhua County. Hunan Geology 11, 1 (in Chinese with English abstract).

Xie, L., Wang, R.C., Groat, L.A., Zhu, J.C., Huang, F.F., Cempírek, J., 2015. A combined EMPA and LA-ICP-MS study of Li-bearing mica and Sn–Ti oxide minerals from the Qiguling topaz rhyolite (Qitianling District, China): the role of fluorine in origin of tin mineralization. Ore Geol. Rev. 65, 779–792. https://doi.org/10.1016/j.oregeorev.2014.08.013.

Xu, J.R., Zhao, Z.X., He, Y.F., Mu, X.Z., 2003. Regional characteristics of stress field and its dynamics in and around Nankai Trough, Japan. Chin. J. Geophys. 46, 488–495 (in Chinese with English abstract).

Yan, H.B., He, J.J., Liu, X.W., Wang, H.B., Liu, J.F., Ding, X., 2020. Thermodynamic investigation of the hydrolysis behavior of fluorozirconate complexes at 423.15–773.15 K and 100 MPa. J. Solution Chem. 49, 836–848. https://doi.org/10.1007/s10953-020-00993-1.

Yang, B.Q., 1989. A brief introduction to Tangqian fluorite deposit, Cailing County. Hun. Geol. 8, 49–53 (in Chinese with English abstract).

Ye, X.F., 2014. Mineralization and metallogenic model of fluorite deposits in the Zhejiang Area. Northwestern Geol. 47, 208–220 (in Chinese with English abstract).

Yuan, J.Q., Zhu, S.Q., Zhai, Y.S., 1979. Mineral Deposits. Geological Publishing House, Beijing, pp. 183–200.

Yuan, S.D., Mao, J.W., Cook, N.J., Wang, X., Liu, X.F., Yuan, Y.B., 2015. A late cretaceous tin metallogenic event in nanling W-Sn metallogenic province: constraints from U-Pb, Ar-Ar geochronology at the Jiepailing Sn-Be-F deposit, Hunan, China. Ore Geol. Rev. 65, 283–293. https://doi.org/10.1016/j.oregeorev.2014.10.006.

Yuan, S.D., Peng, J.T., Hu, R.Z., Bi, X.W., Qi, L., Li, Z.L., Li, X.M., Shuang, Y., 2008. Characteristics of rare-earth elements (REE), strontium and neodymium isotopes in hydrothermal fluorites from the Bailashui tin deposit in the Furong ore field, southern Hunan Province, China. Chin. J. Geochem. 27, 342. https://doi.org/10.1007/s11631-008-0342-5.

Zeng, G., He, Z.Y., Li, Z., Xu, X.S., Chen, L.H., 2016. Geodynamics of paleo-Pacific plate subduction constrained by the source lithologies of Late Mesozoic basalts in southeastern China. Geophysical Research Letters 43, 10,189-10,97. 10.1002/2016GL070346.

Zhang, D.L., Peng, J.T., Fu, Y.Z., Peng, G.X., 2012. Rare-earth element geochemistry in Ca-bearing minerals from the Xianghuapu tungsten deposit, Hunan Prpvince, China. Acta Petrol. Sin. 28, 65–74 (in Chinese with English abstract).

Zhang, K., Hu, J.L., 2012. Geochemistry of Granite and Its Relationship with Mineralization in Taolin Pb-Zn Deposit,Hunan Province. Geology & Mineral Resources of South China 28, 307-14(in Chinese with English abstract). 10.3969/j.issn.1007-3701.2012.04.004.

Zhang, L.P., Hu, Y.B., Liang, J.L., Ireland, T., Chen, Y.L., Zhang, R.Q., Sun, S.J., Sun, W.D., 2017a. Adakitic rocks associated with the Shilu copper–molybdenum deposit in the Yangchun Basin, South China, and their tectonic implications. Acta Geochim. 36, 1–19. https://doi.org/10.1007/s11631-017-0146-6.

Zhang, W., Zhou, L., Tang, H.F., Li, H.P., Song, W.L., Xie, G., 2017b. The solubility of fluorite in Na-K-Cl solutions at temperatures up to 260 °C and ionic strengths up to 4 mol/kg H2O. Appl. Geochem. https://doi.org/10.1016/j.apgeochem.2017.04.017.

Zhang, Y., Han, R.S., Ding, X., He, J.J., Wang, Y.R., 2019. An experimental study on metal precipitation driven by fluid mixing: implications for genesis of carbonate-hosted lead–zinc ore deposits. Acta Geochim. 38, 202–215. https://doi.org/10.1007/s11631-019-00314-4.

Zhang, Y., Han, R.S., Ding, X., Wang, Y.R., Wei, P.T., 2020. Experimental study on fluid migration mechanism related to Pb-Zn super-enrichment: implications to mineralization mechanisms of the Pb-Zn deposits in the Sichuan-Yunnan-Guizhou, SW China. Ore Geol. Rev. 114, 103110 https://doi.org/10.1016/j.oregeorev.2019.103110.

Zhang, Y.J., 1995. Trend and law of fluorite forming fluid migration in cretaceous Wuyi basin, Zhejiang. J. Chengdu Inst. Technol. 22, 86–91 (in Chinese with Ehglish abstract).

Zhao, P.L., Yuan, S.D., Yuan, Y.B., 2016. Zircon LA-MC-ICP-MS U-Pb dating of the Xianglinpu granites from the Weijia tungsten deposit in southern Hunan Province and its implications for the Late Jurassic tungsten metallogenesis in the westernmost Nanling W-Sn metallogenic belt. GEOLOGY IN CHINA 43, 120-31(in Chinese with English abstract). 10.3969/j.issn.1000-3657.2016.01.009.

Zhao, W.W., Zhou, M.F., Li, Y.H.M., Zhao, Z., Gao, J.F., 2017. Genetic types, mineralization styles, and geodynamic settings of Mesozoic tungsten deposits in South China. J. Asian Earth Sci. 137, 109–140. https://doi.org/10.1016/j.jseaes.2016.12.047.

Zhong, J., Pirajno, F., Chen, Y.J., 2017. Epithermal deposits in South China: Geology, geochemistry, geochronology and tectonic setting. Gondwana Res. 42, 193–219. https://doi.org/10.1016/j.gr.2016.10.008.

Zhou, X.M., Li, W.X., 2000. Origin of Late Mesozoic igneous rocks in Southeastern China: implications for lithosphere subduction and underplating of mafic magmas. Tectonophysics 326, 269–287. https://doi.org/10.1016/S0040-1951(00)00120-7.

Zhou, X.M., Sun, T., Shen, W.Z., Shu, L.S., Niu, Y.L., 2006. Petrogenesis of Mesozoic granitoids and volcanic rocks in South China: A response to tectonic evolution. Episodes 29, 26–33. https://doi.org/10.1007/s00254-006-0175-7.

Zhu, J.C., Zhang, P.H., Xie, C.F., Zhang, H., Yang, C., 2006. Ziucon U-Pb age framework of Huashan-Guposhan intrusive belt, western part of Nanling Range, and its geological significance. Acta Petrologica Sinica 22, 2270-8(in Chinese with Ehglish abstract). 10.3969/j.issn.1000-0569.2006.09.002.

Zhu, X.Y., Wang, J.B., Wang, Y.L., Cheng, X.Y., Fu, Q.B., 2012. The geochemical study of the S-Pb isotope in the W-Mo -Bi-Pb-Zn polymetallic deposit in Huangshaping, Hunan Province. Acta Petrol. Sin. 28, 3809–3822 (in Chinese with English abstract).

Zou, H., Mary, R., Liu, Y.S., Yao, Y.P., Xu, X.S., Fan, Q.C., 2003. Constraints on the origin of historic potassic basalts from northeast China by U-Th disequilibrium data. Chem. Geol. 200, 189–201. https://doi.org/10.1016/S0009-2541(03)00188-8.

Zou, H., Zhang, Q., Bao, L., Fang, Y., 2016. Geological characteristics and ESR dating of Xiachen fluorite deposit in Tiantai basin,Zhejiang,China. Journal of Chengdu University of Technology(Science & Technology Edition) 43, 86-94(in Chinese with English abstract). 10.3969/j.issn.1671-9727.2016.01.09.